$La_{2/3}Ca_{1/3}MnO_3$ Nanoparticles with Novel Magnetoresistance Property

Jianwu Zhang,[1] Eue-Soon Jang, Il-Won Chung,[2] and Jin-Ho Choy*

National Nanohybrid Materials Laboratory (NNML), School of Chemistry and Molecular Engineering, Seoul National University, Seoul 151-747, Korea
Received August 28, 2003

Fine $La_{2/3}Ca_{1/3}MnO_3$ nanocrystalline powders have been successfully prepared by modified citrate pyrolysis process. The obtained LCMO nanoscale grains have a mean particle size of about 30 nm under optimal treatment conditions. The particle size can be controlled by adjusting processing parameters, such as treatment temperature and calcination time. X-ray diffraction, SEM and magnetoresistance effect were employed to study the crystal structure, morphology and magnetic property of these nanosized powders. A novel MR effect (MR > 45% (0 K < T < 340 K)) at room temperature has been found.

Key Words : $La_{2/3}Ca_{1/3}MnO_3$ nanoparticles, Citrate pyrolysis process, Magnetoresistance effect

Introduction

The technological interest in Ca-doped $LaMnO_3$ as a colossal magnetoresistance (CMR) perovskite has been rapidly increasing because of the possible application of Ca-doped $LaMnO_3$ for highly dense data storage, magnetically sensitive sensors, and solid fuel cell electrodes.[1-3] In particular, synthesis of $La_{1-x}Ca_xMnO_3$ (LCMO) nanoparticles is very important not only for fabricating electrodes and thin film, but also for understanding the CMR phenomenon.[4,5] However, obtaining the LCMO nanoparticles through the conventional solid-state reaction is very difficult since a temperature of more than 1200 °C is usually required to achieve the LCMO crystal with single phase. This extreme condition could induce an increase of particle size up to several tens micrometer scale.[6-8]

Although the citrate pyrolysis method is the most suitable procedure to overcome the above problem, only a few attempts have been tried because the LCMO crystals have three different metals, and thus homogeneous stoichiometric composition is not easily obtain through citrate pyrolysis.[9-11]

In the present paper, we present the successful synthesis of LCMO nanoparticles by modified citrate pyrolysis. In addition, the systematic study of the resulting LCMO nanoparticles was achieved through the direct observation of morphology and characterization of magnetic property.

Experimental Section

First, the stoichiometric amounts of La_2O_3, $CaCO_3$, and MnO_2 were mixed thoroughly in an agate mortar, and then the resulting precursor was dissolved in a nitric acid solution at about 80 °C. Second, 0.33 mole of citric acid and 0.1 mole of ethylene glycol were dissolved in de-ionized water and then mixed with the above nitric acid solution. Under continuous stirring, the resulting solution was heated to 90-100 °C until it turned into a brown colored gel. And then a dark-brown resin was obtained from the brown gel by drying at 150 °C for 24 hours in a vacuum oven. Finally, the resulting resin was pulverized and then calcined at various temperatures to optimize synthetic condition of the LCMO nanoparticles, as shown in Table 1. To compare with bulk crystal, the LCMO crystal was prepared by the conventional solid state procedure.

Table 1. The lattice parameters of the samples prepared under different conditions

Lattice Parameter	S600	S700	S800	S1300	S1400
a (Å)	7.7057	7.7124	7.7067	7.7355	7.7306
b (Å)	7.6995	7.7126	7.6883	7.7352	7.7230
c (Å)	7.7018	7.6999	7.7147	7.7286	7.7300
Cell Volume ($Å^3$)	456.9480	458.0105	457.1069	462.4457	461.5075

The phase characterization of the resulting products was made by X-ray diffraction (XRD) analysis using a Philips PW 1830 powder diffractometer with Ni-filtered Cu-K_α radiation (λ_α = 1.54187 Å). The mean crystallite size was calculated from the X-ray line broadening of the (100) diffraction peak, using the Scherrer formula, $D = 0.89\ \lambda / B\cos\theta$, where D is the crystallite size in nm, λ is the radiation wavelength, θ is the diffraction peak angle and B is the corrected line with width at half-peak intensity.[12] The correction for instrumental peak broadening was made using the Warren formula: $B = (b^2_{obs} - b^2)^{1/2}$, where b_{obs} is the line width at half-peak intensity related to LCMO, and b is the line width of the (202) diffraction peak of the metallic silicon, which is used as an internal standard. The d-values of the samples were determined from the X-ray diffraction peaks by a standard least-squares refinement method with an error less than 0.1%. The morphology was observed by the field emission scanning electron microscopy (FE-SEM, Hitach S-4300). The susceptibility and magnetoresistance

*Corresponding author: Tel: +82-2-880-6658; Fax: +82-2-872-9864; e-mail: jhchoy@snu.ac.kr
Present address: [1]Structure Research Laboratory, Department of Physics, University of Science and Technology of China, Hefei 230026, P.R. China. [2]Department of Naval Academy 645-797, Korea

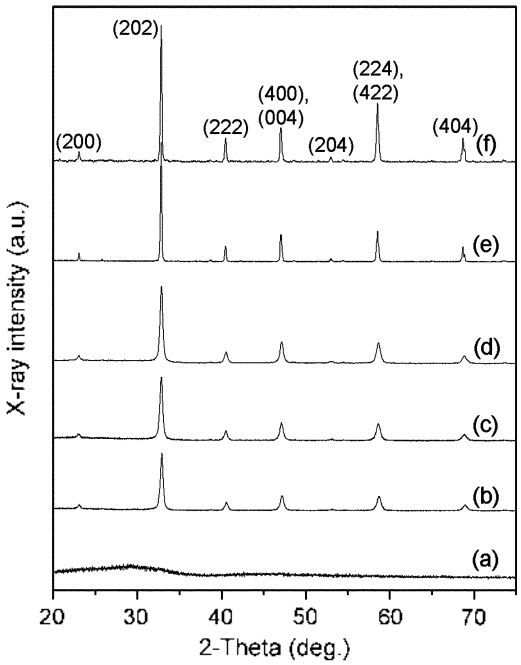

Figure 1. XRD patterns of the $La_{2/3}Ca_{1/3}MnO_3$ crystals heated at (a) 500 °C/1 hr, (b) 600 °C/1 hr, (c) 700 °C/1 hr, (d) 800 °C/2 hrs, (e) 1,300 °C/20 hrs, and (f) 1,400 °C/48 hrs.

(MR) effect were measured with a Quantum Design SQUID magnetometer under zero-field-cooled (ZFC) and field cooled (FC) conditions with an applied magnetic field.

Results and Discussion

While the LCMO sample heated at 500 °C for 1 hr was characterized as an amorphous phase in the XRD pattern, the LCMO single phases were successfully achieved by heating beyond 600 °C, as shown in Figure 1. In addition, the full width half maximum (FWHM) of X-ray diffraction peaks for LCMO heated at 600-800 °C is larger than that for the product heated at 1,300-1,400 °C. This fact indicates that the mean size of the former is smaller than that of the latter. The average particle size was determined as 24.5 nm for the sample treated at 600 °C for 1hr, and 21.0 nm at 700 °C for 1 hr, and 23.7 nm at 800 °C for 2 hrs by the Scherrer Formula. As shown in Table 1, the unit cell volumes determined from X-ray diffraction patterns are fully consistent with the above result, which indicates that LCMO nanoparticles could be synthesized through the present procedure only by heating at lower temperature of 600 °C, compared with the conventional solid state process at 1400 °C.

As shown in Figure 2(a), the LCMO nanoparticles heated at 700 °C for 1hr exhibit a homogeneous spherical shape with an average size of 30 nm, which is in good agreement with XRD analysis. Figure 2(b) shows that the LCMO crystal obtained from the conventional solid state reaction (1400 °C/48 h) has a mean particle size of 20 μm, which is remarkably larger than that of the present LCMO nanoparticles.

Figure 3(a) and (b) show the temperature dependence

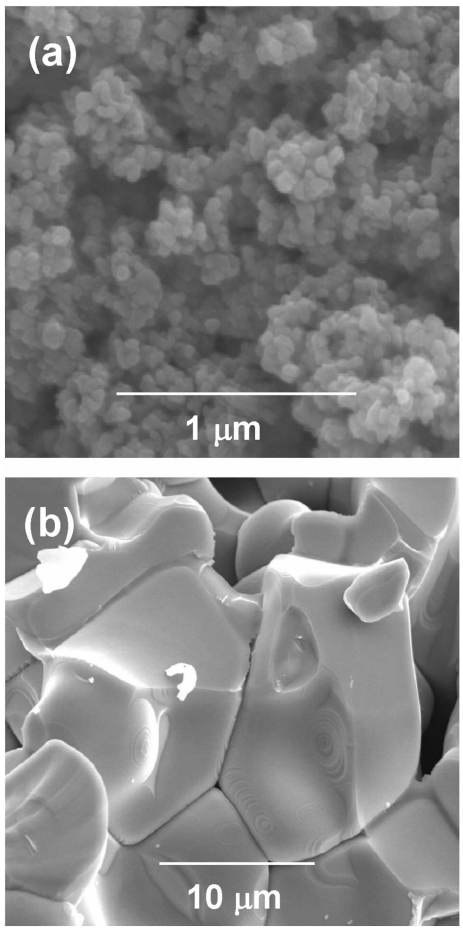

Figure 2. The FE-SEM images of (a) the S700 nanoparticles and (b) the S1400 bulk crystals.

resistivity for the heated samples at 700 °C for 1 hr and 1,400 °C for 48 hrs (hereafter referred to as S700 and S1400) under various applied fields from zero field to 5 T. As shown in Figure 3(a), a metal-semiconductor (M-S) crossover is observed at 140 K for the sample of S700, whose M-S transition temperature is shifted to a higher temperature with an increase of applied field from 0 T to 5 T, as indicated with a solid arrow. When the temperature decreases down to 50 K, the resistivity increases significantly as shown in Figure 3(a). This indicates that the conducting state of S700 is changed again from metal to semiconductor at low temperature. On the contrary, the M-S crossover in S1400 is observed at 245 K, and its M-S transition is not further observed at low temperature as shown in Figure 3(b). Therefore, the second M-S transition for S700 nanoparticles at low temperature could be explained by a charge localized behavior through small grain boundary effect rather than a frozen-in magnetic disorder.[13]

Figure 4(a) and (b) show MR *vs* temperature for the samples of S700 and S1400, respectively. Surprisingly, a novel MR effect (MR > 45% (0 K < T < 340 K)) appears for S700, which is significantly different from that for S1400. Such a distinctive MR effect could be explained by two main factors such as the magnetic disorder effect at the interface and surface of LCMO nanoparticles and the tunneling effect

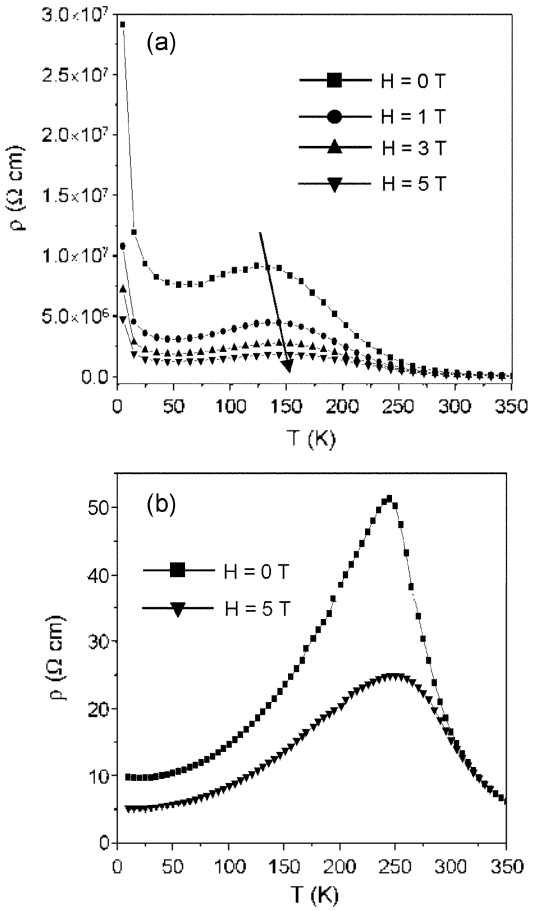

Figure 3. The temperature dependence of resistivity for (a) the S700 and (b) S1400 upon applied magnetic field.

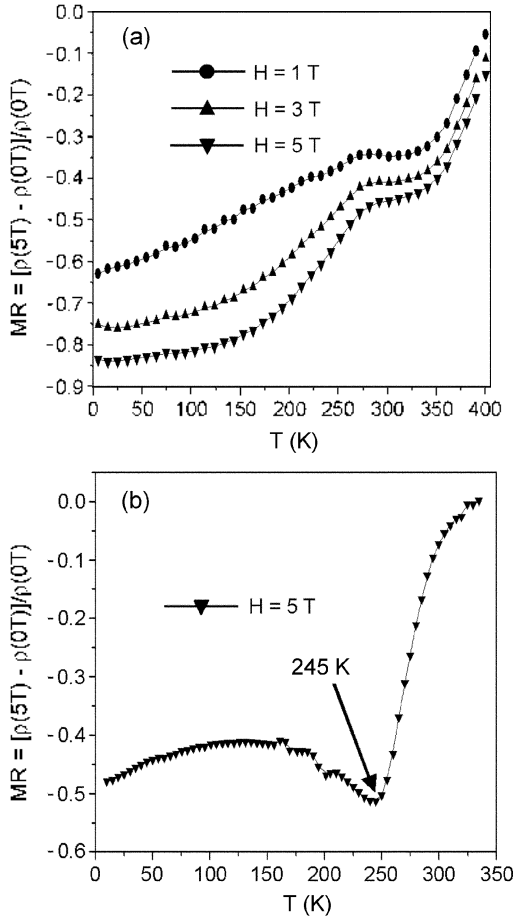

Figure 4. The temperature dependence of magnetoresistance (MR) for (a) the S700 and (b) S1400.

of electrons between nanoparticles.[14,15]

On the one hand, when an external magnetic field is applied, Mn spins within disordered region would be re-aligned along the field direction, and as a consequence the electron tunneling rate among LCMO grains could be facilitated, and thus MR increases; in other words, the magnetic disorder would decrease, and thus weaken the magnetic scattering of charge carriers, finally giving rise to the enhancement of MR.

Conclusion

The LCMO nanoparticles were successfully synthesized by modified citrate pyrolysis. The LCMO nanoparticles prepared at 700 °C for 1 hr have a mean particle size of about 30 nm, which can easily be controlled by adjusting the processing parameters, such as reaction temperature and calcination time. A novel MR effect (MR > 45% (0 K < T < 340 K)) at room temperature has been found for the first time in the present LCMO nanoparticles.

Acknowledgements. This work is financially supported by the Korean Ministry of Science and Technology (NRL project99) and by the Ministry of Education (BK 21 program).

References

1. Taimatsu, H.; Wada, K.; Kaneko, H.; Yamamura, H. *J. Am. Ceram. Soc.* **1992**, *75*, 401.
2. Hong, C. S.; Kim, W. S.; Chi, E. O.; Lee, K. W.; Hur, N. H. *Chem. Mater.* **2000**, *12*, 3509.
3. Akther Hossain, A. F. M.; Cohen, L. F.; Berenov, A.; Macmanus Driscoll, J. L. *Mater. Sci. & Eng. B* **2000**, *77*, 261.
4. Hawley, M. E.; Adams, C. D.; Arendt, P. N. *J. Cryst. Growth* **1997**, *174*, 455.
5. Mukovskii, Y. M.; Shmatok, A. V. *J. Magnetism & Magnetic Mater.* **1999**, *196*, 136.
6. Choy, J.-H.; Hong, S.-T. *Bull. Korean Chem. Soc.* **1991**, *12*, 349.
7. Choy, J.-H.; Hong, S.-T.; Park, N.-G.; Byeon, S.-H.; Demazeau, G. *Bull. Korean Chem. Soc.* **1995**, *16*, 105.
8. Chi, E. O.; Kang, J.-K.; Kwon, Y.-U.; Hur, N. H. *Bull. Korean Chem. Soc.* **1997**, *18*, 1238.
9. Roosmalen, J. A. M.; Cordfunke, E. H. P.; Huijsmans, J. P. P. *Solid State Ionics* **1993**, *66*, 285.
10. Choy, J.-H.; Han, Y.-S. *Mater. Lett.* **1997**, *32*, 209.
11. Hueso, L. E.; Rivas, J.; Rivadulla, F.; Lopez-Quintela, M. A. *J. Appl. Phys.* **1999**, *86*, 3881.
12. Cullity, B. D. *Elements of X-ray Diffraction*; Addison-Wesley: Reading, 1978; p 102.
13. Balcells, L.; Fontcuberta, J.; Martinez, B.; Obradors, X. *Phys. Rev. B* **1998**, *58*, R14697.
14. Hwang, H. Y.; Cheong, S.-W.; Ong, N. P.; Batlogg, B. *Phys. Rev. Lett.* **1996**, *77*, 2041.
15. Li, X. W.; Gupta, A.; Xiao, G.; Gong, G. Q. *Appl. Phys. Lett.* **1997**, *71*, 1124.